Regular Article

PHYSICAL CHEMISTRY RESEARCH
Published by the
Iranian Chemical Society
www.physchemres.org
info@physchemres.org

***Phys. Chem. Res.**, Vol. 7, No. 2, 375-394, June 2019*
DOI: 10.22036/pcr.2019.156619.1565

Tautomerism, Intramolecular H-bonding, Acidity and Complexation of 2,4-Dioxo-4-Phenylbutanoic Acid

E. Khalilinia and A. Ebrahimi*

Department of Chemistry, University of Sistan and Baluchestan, P. O. Box: 98167-45845, Zahedan, Iran

(Received 17 November 2018, Accepted 1 April 2019)

In this work, the properties of 2,4-dioxo-4-phenylbutanoic acid (DPBA) and some of its derivatives have been investigated using quantum mechanical calculations in the gas phase and solution media. The electron delocalization and intramolecular H-bonds substantially affect the potential energy surface. At all levels of calculations and phases (gas and three solutions) selected in this work, enolic tautomers are more stable than diketo, and the repulsive H···H interaction and the orientation of double bonds affect the relative stability of enolic tautomers. The trend does not change in the presence of substituents located on the phenyl group. The acidity of the most stable enolic tautomer is lower than that of the other two tautomers. The effect of solvent on the acidities of tautomers was investigated by explicitly introducing the molecules, and implicitly introducing them as a uniform environment. Although the acidity of enolic group is higher than that of carboxylic group in the gas phase, the order is reversed in the aqueous solution using both methods. The order of acidities of tautomers depends on the phase and substituents; increases in the acidity and the trend of acidities of tautomers change after complexation with Mg^{2+}.

Keywords: 2,4-Dioxo-4-phenylbutanoic acid, Hydrogen bonding, Population analysis, Acidity, Complexation

INTRODUCTION

Diketo acids (DKAs) with one carboxyl and two carbonyl groups are very attractive in different of chemistry [1-3]. The mentioned functional groups make DKAs and their derivatives chemically and biologically active, and important in drug design programs. The screening of a library of 200,000 compounds by a team of Italian researchers [4,5] has shown that DKAs and some of their derivatives can function as selective and reversible inhibitors of hepatitis C virus RNA-dependent RNA polymerase (RdRP HCV, viral nonstructural protein NS5b). In addition, it has been shown that 2,4-DKA derivatives can be beneficial in building several angiotensin-converting-enzyme (ACE) inhibitors [6].

The inhibitory effects of DKAs and related compounds on the HIV-1 integrase (IN) have also been investigated by many authors [7-13] Sechi *et al.*, designed and synthesized some DKA complexes when they examined the metal-complexing ability of some DKAs in solution media. They used the lipophilic balance, by complexation with the metal ions, in order to explain different antiviral potencies of certain DKA compounds with similar physicochemical properties [9]. On the other hand, there are some serious problems in the synthetic methodology required to produce a structurally diverse family of new DKAs with interest in HIV integrase inhibitors [19]. However, a novel strategy has been used to assemble the β-DKA pharmacophore of HIV integrase inhibitors on purine nucleobase scaffolds [10]. Some witnesses show that among all reported IN inhibitors, some β-DKAs that have entered the clinical trials are the most promising compounds [20-23].

The 2,4-dioxo-4-phenylbutanoic acid (DPBA), which is a β-DKA, has been studied extensively as a drug for hepatitis C [4,24-26], HIV-1 [7-12] and influenza [27-30].

*Corresponding author. E-mail: ebrahimi@chem.usb.ac.ir

Some works have also been performed on novel DPBA analogs as mycobacterium tuberculosis inhibitors [31].

The effects of aryl substitutions on the properties of the dioxobutanoic moiety were investigated by Cvijetić *et al.* [32]. In addition, they experimentally studied the effect of pH on the electronic properties of some related compounds. All calculations were performed on the enolic tautomer of DPBA that was specified as predominant using the NMR spectroscopy and cyclic voltammetry [33]. As the study was performed in the presence of CF_3COOD, D-acetate buffer, and H-carbonate buffer, and considering the minor difference between stabilization energies of tautomers, it is expected that the solvents affected the dominant form of DPBA.

The intramolecular H-bonds (IHBs), as the most important intramolecular interactions, have a crucial role in the molecular structures, chemical reactions, and conformational preference of compounds [34,35]. They can affect many molecular features such as the proton transfer phenomenon, crystalline synthons, and molecular structures in the molecular and biomolecular systems [36,37]; hence, the nature of IHBs has been the subject of many experimental and theoretical studies [38-43]. The strong IHBs in the enolic tautomers of β-diketons can be attributed to the π-conjugating skeleton that can be assisted by electron delocalization on six membered rings made by H-bonding [44-46].

In the present work, the relative stability of tautomers of DPBA and the effects of substituents located on the phenyl group were systemically investigated in the gas phase and solutions. In addition, the acidities of carboxylic and enolic hydrogens were investigated in the gas phase and in the presence of solvent explicitly and implicitly, before and after complexation with Mg^{2+}. The complexation with the metal ion and the change in the acidity can critically affect the activity of DPBA as a drug in the body [9,12,14,47]; especially, functional sequestration of Mg^{2+} ion in the active site of HIV-1 integrase can be performed by DPBA, as an aryl diketo acid [33]. The activities of several sites of DPBA on complexation with the Mg^{2+} ion and the effects of substituents located at the six-membered ring on the acidity of DPBA have also been investigated in the gas phase and solution media.

COMPUTATIONAL DETAILS

The density functional theory (DFT) is presently the most successful approach to compute the electronic structure of many-body systems, in particular atoms, molecules, and the condensed phases [48-54]. Herein, full geometry optimization of compounds and complexes were carried out using the M06-2X [55] method in conjunction with the 6-311++G(d,p) basis set using the Gaussian 09 program package [56]. Frequency calculations were also performed at the above-mentioned level to identify the nature of stationary points and to obtain the thermodynamic properties at the same level. In addition to the above mentioned level, the most stable conformers of tautomers were also optimized using the B3LYP-D3 [57], wB97XD [58], and MP2 [59] methods in conjunction with the 6-311++G(d,p) basis set in the gas phase and two solutions. The effects of method and basis set on the stabilities of tautomers in the presence of substituents have also been investigated by single point calculations at the B3LYP/6-311++g(d,p), B3LYP-D3/6-311++G(d,p), and M06-2x/aug-cc-pVDZ levels of theory. The nature of intramolecular hydrogen bonds were identified using the results of the atoms in molecules (AIM) analysis carried out in the AIM2000 software [60,61]. The quantum theory of AIM is a model that characterizes the chemical bonding of systems based on the topology of the electronic charge density. Although this method is a very useful tool in analyzing the hydrogen bonds, it does not reveal the origin of this phenomenon. This problem has been successfully solved by the natural bond orbital (NBO) analysis. The NBO analysis was carried out on the mentioned wave functions using the NBO 3.1 package [62] included in the Gaussian 09 program.

The acidities of DPBA tautomers were estimated using two models: (1) using the ΔG values of reaction indicated in Eq. (1)

$$HA \rightarrow H^+ + A^- \quad (1)$$

These calculations were performed using the M06-2X method in conjunction with the 6-311++G(d,p) basis set by a self-consistent reaction field (SCRF) model; *i.e.*, the integral equation formalism variant of the polarizable

continuum model (IEFPCM) [63], in the water and $CHCl_3$ solvents. (2) eight water molecules were located around each tautomer in chemically rational positions, and the structures were optimized in the gas phase and solution media. Then, the positions of the potentially acidic H atoms were separately scanned from those in the compound toward the nearest water molecules. In other words, the reaction indicated in Eq. (2) was modeled to estimate the acidity and to investigate the kinetics of H^+ exchange between H_2O and selected tautomer.

$$HA + H_2O \leftrightarrows A^- + H_3O^+ \quad (2)$$

RESULTS AND DISCUSSION

Tautomerism and Intramolecular H-bonding

The most probable conformers of three tautomers of DPBA, including one diketonic (series **I**) and two enolic (series **II** and **III**) tautomers, are presented in Fig. 1S. The relative energies of the structures optimized at the M06-2X/6-311++G(d,p) level of theory are given in Fig. 1S, too. As can be seen, the most stable conformers of the series **I** and **III** are local minima, and the most stable conformer of the series **II** is the global minimum on the potential energy surface. As seen in Scheme 1, two parameters can be used as indicators for planarity; the inter-ring torsion angle Φ ($=D_{C4C2C1C3}$) and the difference between the adjacent C-C double and single bond lengths between acceptor and π moieties (Δr), which the latter is shown in bold lines in Scheme 1. An inter-ring torsion angle below 1° and small difference between neighboring C-C bonds demonstrate the high planarity which is desirable for achieving effective π-conjugation [64]. The Φ (and Δr) values are 0.29, 0.09, and 0.43 degrees (0.09, 0.07 and 0.09 Å) in **I**, **II** and **III**, respectively. Given the values of Φ, Δr and the dihedral angle θ ($=D_{C4C5C6C7}$), **II** and **III** are planer, but **I**, in which $\theta = 70°$, is not planar.

The results of calculations at various levels of theory on the most stable conformers of tautomers in the gas phase and two solutions are given in Table 1. At all levels and all media, the most stable structure corresponds to **II**, and the order of stability is **II** > **III** > **I**. The tautomer **III** has been estimated more stable than **II** in the Verbić *et al.*'s work [33]. This difference in the relative stabilities of the tautomers **II** and **III** can be attributed to the difference in the solvent and the slight difference in the stabilization energies of tautomers **II** and **III**. The differences in the stabilization energies of **II** and **III** are in the ranges 1.5-5.7 and 0.1-3.6 and 0.5-4.4 kcal mol^{-1} at various levels in the gas phase, water, and $CHCl_3$, respectively.

Two typical isodensity surfaces obtained from AIM analyses for enolic tautomers are shown in Fig. 1. As can be seen, the conjugated double bonds and delocalization of π-electronic cloud support planarity in the enolic tautomers **II** and **III**. Delocalization of π-electrons in diketo tautomer is lower than that in other tautomers; this phenomenon and high angle strain make the side chain out of plane in tautomer **I**. The strong C=O···H hydrogen bonds (r = 1.69-2.00 Å) and weak H···H interactions (r = 2.0-2.10 Å) are only observed in planar structures of enolic tautomers, and the former makes tautomers **II** and **III** more stable than **I**.

The difference between the stabilities of two enolic tautomers decreases (see Table 1) from the gas phase to the solution and with the increase in dielectric constant of solvent, which can be related to the extra stabilization of more polar compounds in the water. It is equal to 1.94, 1.71, and 1.58 kcal mol^{-1} in the gas phase, $CHCl_3$, and water, respectively, at the M06-2X/6-311++G(d,p) level.

The electronic charge densities (ρ) and the Laplacian of electronic charge densities ($\nabla^2\rho$), calculated at the H-bond critical points (HBCPs) using the AIM analysis on the wave functions obtained at the M06-2X/6-311++G(d,p) level, are given in Table 2. In addition, this table includes the most important geometrical parameters of related H-bonds and the donor-acceptor interaction energies $E^{(2)}$ obtained from the NBO analysis.

Two H···O H-bonds are observed from the structural parameters and the results of AIM and NBO analyses in the enolic tautomers **II** and **III**, one of which is a resonance-assisted [65] strong OH···O H-bond (RAHB). As can be seen in Table 2, the $E^{(2)}$ values of $lpO \rightarrow \sigma^*OH$ interaction of OH1···O and O···H1O are higher than those of O···H2O in enolic tautomers **II** and **III**, respectively. The values for O···H1O and O···H2O are respectively equal to 34.6 and 2.11 kcal mol^{-1} in **III**, and for OH1···O and O···H2O are 24.3 and 3.84 kcal mol^{-1} in **II**. The ρ (and $\nabla^2\rho$) values calculated at the HBCP of the mentioned interactions are

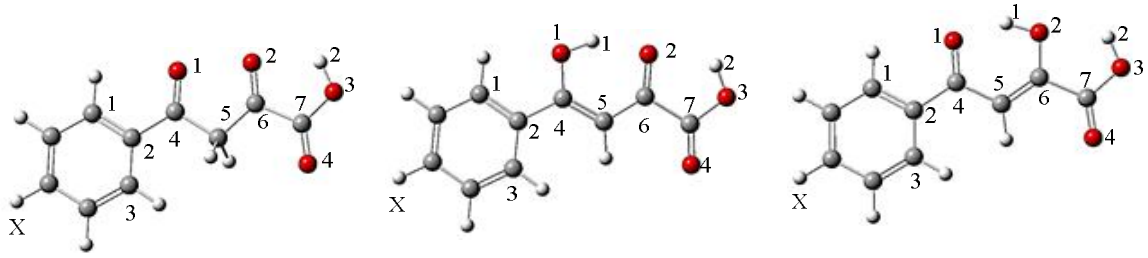

I **II** **III**

φ = 0.29 °, Δr = 0.09 Å φ = 0.09 °, Δr = 0.07 Å φ = 0.43°, Δr = 0.09 Å

X = NH_2, OH, OCH_3, CH_3, H, F, Cl, Br, CN, NO_2

Scheme 1. Diketo **I** and enolic tautomers **II** and **III** of 2,4-dioxo 4-phenyl butanoic acid. Δr (= r_{C2C4}-r_{C2C3}) is the difference between the adjacent C-C double and single bond lengths between acceptor and π moieties, and Φ (=DC4C2C1C3) is the inter-ring torsion angle

Table 1. The Relative Energies (in kcal mol^{-1}) of Tautomers Calculated at the Four Levels

	B3LYP-D3			M06-2X		
	I-II	III-II	E_{II}	I-II	III-II	E_{II}
Gas	8.19	2.46	-687.03472	7.14	1.94	-686.63919
Water	5.83	2.24	-687.04622	3.33	1.58	-686.72689
$CHCl_3$	6.71	2.35	-687.04304	4.23	1.71	-686.72367
	wB97XD			MP2		
Gas	5.45	2.23	-686.75301	3.35	1.83	-685.14103
Water	2.91	1.89	-686.76388	1.43	1.52	-685.15088
$CHCl_3$	3.83	2.03	-686.76068	2.13	1.63	-685.14796

respectively equal to 5.8×10^{-2} (1.52×10^{-1}) and 2.3×10^{-2} (1.08×10^{-1}) au in tautomer **III**. The values are respectively equal to 4.8×10^{-2} (1.48×10^{-1}) and 2.6×10^{-2} (1.08×10^{-1}) au in tautomer **II**. The ρ_{HO} and $E^{(2)}_{lpO \rightarrow \sigma^*(OH)}$ parameters can be used as measures to compare the strength of H-bonds in the tautomers. Thus, OH1···O and O···H1O are much stronger than O···H2O in the enolic tautomers, which can be attributed to the positions of atoms in the enolic tautomers and the orientations of molecular orbitals contributed to the interactions. The OH1···O and O···H1O bonds form a six-membered ring in both tautomers, which is a more appropriate distance and orientation available for H-bond interaction, while the O···H2O bond forms a five-membered ring.

Considering the structural parameters and the results of AIM and NBO analyses, the O···H1O bond in **III** is considerably stronger than that (OH1···O) in **II**. Resonance with the phenyl group makes O1 a more electron donor and the mentioned H-bond stronger in tautomer **III**.

The O2 atom participates in two intramolecular interactions as H-bond acceptor in tautomer **II**, while it participates in one H-bond interaction as acceptor in **III**. In other words, besides H1···O2, the lone pairs of O2 participate in the O2···H2 H-bond lowering its tendency in the former interaction in tautomer **II**. The latter interaction makes the tendency of H1 stronger in the O1···H1 H-bond in

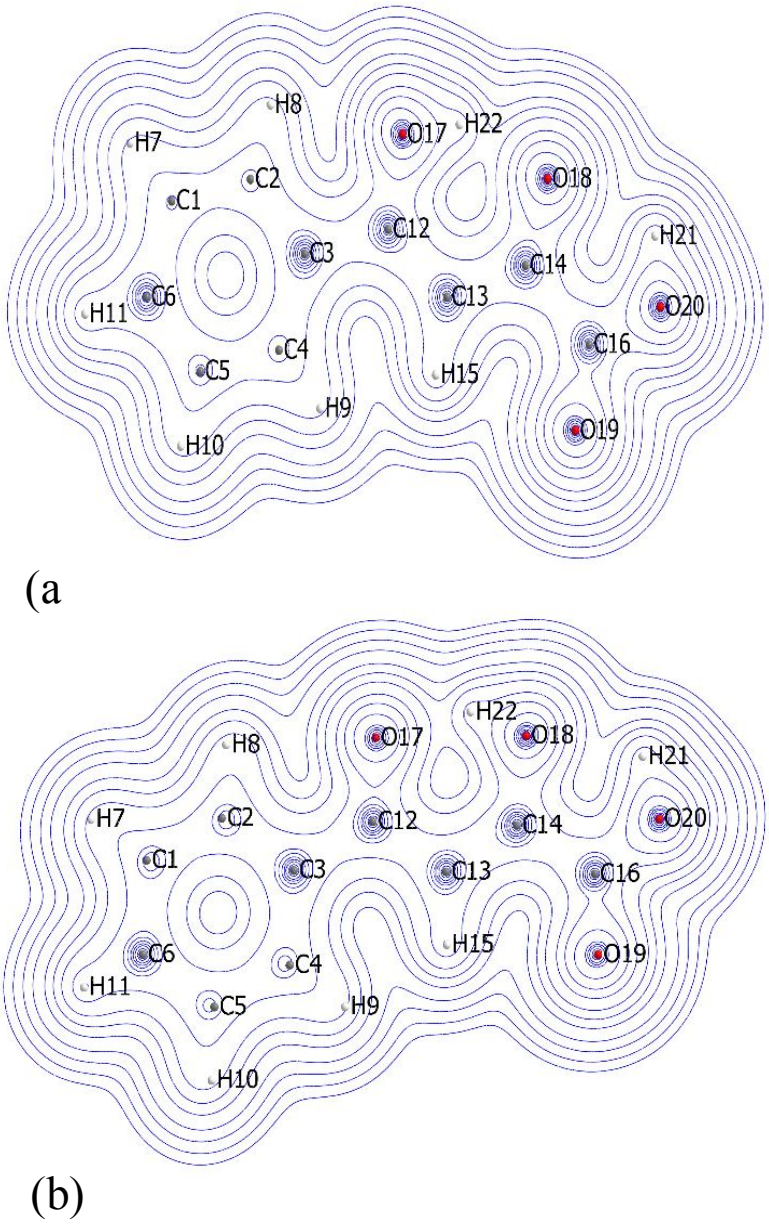

Fig. 1. The isodensity surfaces obtained from AIM analysis for (a) tautomer **II** and (b) tautomer **III**.

tautomer **III**. These make the O···H1O intramolecular interaction in **III** stronger than OH1···O in **II**. This description is confirmed by the rotation of carboxyl group around the C6C7 bond, which breaks the second H-bond in **II**.

Although these results support the stronger H-bond in the tautomer **III**, the more stable tautomer is **II**. The AIM analysis shows that there is a H···H repulsive interaction with $\rho = 1.17 \times 10^{-2}$ and $\nabla^2\rho = 4.48 \times 10^{-2}$ a.u. in tautomer **III**, and 1.13×10^{-2} and 4.44×10^{-2} au in **II**. The stronger repulsive interaction in **III** makes it slightly less stable than **II**. In addition, the conjugated system is more extended in tautomer **II** as compared with **III**.

The OH···O intramolecular H-bonds are also observed

Table 2. The Topological Electron Charge Densities ($\times 10^2$ in a.u.), Donor-acceptor Interaction Energies (in kcal mol^{-1}), and the Lengths (in Å) of H-bonds of Enolic Tautomers Calculated at the M06-2X/6-311++G(d,p) Level

	H-bond	r	ρ	$\nabla^2 \rho$	$E^{(2)}$
II	OH1···O	1.69	4.8	1.48	19.82 + 4.48
	O···H2O	2.01	2.6	1.08	0.86 + 2.98
	H···H	2.10	1.1	0.44	
III	O···H1O	1.62	5.8	1.52	29.73 + 4.87
	O···H2O	2.01	2.3	1.08	2.11
	H···H	2.01	1.2	0.44	

Table 3. The Relative Energies (in kcal mol^{-1}) of Tautomers in the Presence of Substituents Calculated at the M06-2x/6-311++G(d,p) Level

X	[1]**I**	[1]**III**	[2]**II**	X	**I**	**III**	**II**
NH_2	6.11, **3.78**	1.85, **1.65**	7.92417, **7.90836**	F	5.76, **3.32**	1.73, **1.44**	-35.95770, **-35.96880**
OH	5.80, **3.45**	1.77, **1.53**	-11.94270, **-11.95770**	Cl	5.78, **3.35**	1.78, **1.49**	53.68406, **53.67326**
OCH_3	5.92, **3.54**	1.88, **1.61**	-51.23160, **-51.24440**	Br	5.82, **3.39**	1.81, **1.52**	-60.28740, **-60.29830**
CH_3	5.89, **3.45**	1.88, **1.58**	23.97609, **23.96519**	CN	5.87, **3.52**	1.83, **1.56**	-28.9515, **-28.96700**
H	5.86, **3.44**	1.92, **1.60**	63.28401, **63.27326**	NO_2	5.90, **3.62**	1.87, **1.59**	-141.20200, **-141.21700**

1) $RE = E_i - E_{II}$, where i = **I** or **III**. 2) $750 + E_{II}$ in Hartree, with the exception of Cl (with $1200 + E_{II}$) and Br (with $3200 + E_{II}$). 3) The bold data were calculated at the solution media.

for diketonic tautomer **I**. These interactions are weaker than those of **II** and **III** because of the nonplanar structure, improper orientation of H-bond donor and acceptor, and the absence of resonance in the tautomer **I**.

The stabilities of tautomers were also compared in the presence of substituents located at the six-membered ring at several levels of theory in the gas phase and solutions. The relative energies of tautomers **I** and **III**, in comparison to the most stable tautomer **II**, calculated in the gas phase and solution media using the B3LYP, B3LYP-D3, and M06-2X methods in conjunction with the 6-311++G(d,p) and ccPVDZ basis sets, are listed in Tables 3 and 1S (in supplementary materials). The differences in the stabilization energies $E_{I\text{-}II}$ (and $E_{III\text{-}II}$) change slightly by changing the method and basis set. They change from ~ 6.0 (1.8) at M06-2x/6-311++G(d,p) to 9.5 (2.6) kcal mol^{-1} at the B3LYP/6-311++G(d,p) level. The differences decrease in the solution media. The $E_{I\text{-}II}$ ($E_{III\text{-}II}$) values decrease at most by 2.5 (0.3) kcal mol^{-1} from the gas phase to the water solvent at the M06-2x/6-311++G(d,p) level. However, the difference in the stabilization energies of **II** and **III** in the presence of various substituents is less than 4.5 (2.5) kcal mol^{-1} in the gas phase (solution) and the trend in the relative stabilities does not change by substituents.

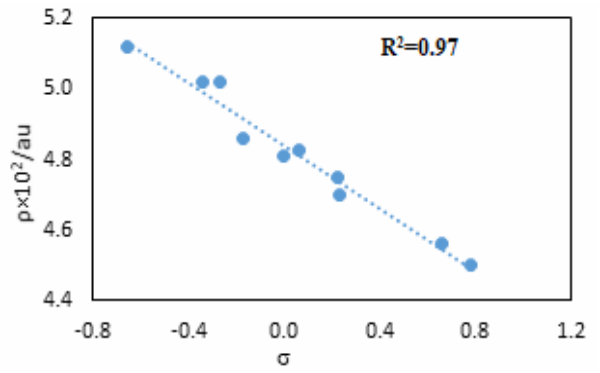

Fig. 2. Correlation between Hammett constants and the ρ values for OH1···O H-bond in tautomer **II**.

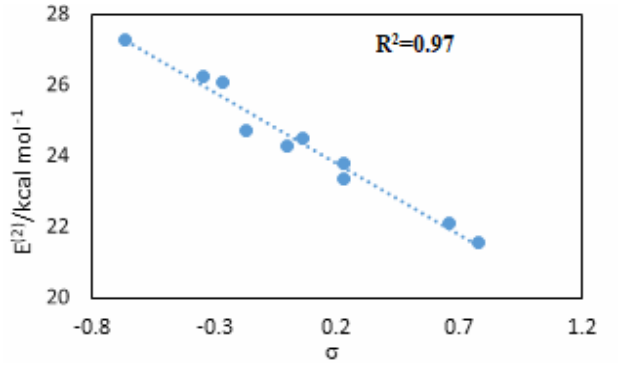

Fig. 3. Correlation between the σ constants of substituents and the $E^{(2)}$ values for OH1···O H-bond in tautomer **II**.

As can be seen in Table 3, the $RE_{i\text{-}II}$ (i = **I** and **III**) values decrease in the presence of EWSs, while they often increase in the presence of EDSs. The ED and EW substituents strengthen/weaken the H-bonds in both tautomers **II** and **III**. The resonance between phenyl group and the six-membered ring made by H-bond decreases/increases in presence of EWSs/EDSs. The effect of resonance on the stability of **II** is higher than that of **III**. Therefore, increase/decrease in the relative energy level of **II** is bigger than those of **I** and **III** in the presence of EWSs/EDSs.

Increase in the electron density around the H-bond acceptor reinforces the ρ_{HO} and $E^{(2)}_{lpO \rightarrow \sigma^*(OH)}$ parameters. According to Table 2S, it is obviously found that the both parameters increase/decrease in the presence of ED/EW substituents.

The Hammette constants σ of substituents located at the ring are negative for NH_2, OH, OCH_3 and CH_3 substituents, and are positive for Br, Cl, F, CN and NO_2 substituents [66]. The σ constants of substituents are in good linear relationship with the ρ values calculated at the O···H BCPs and the $E^{(2)}$ values of lpO → σ*(OH) (are given in Table 2S), where the correlation coefficients are equal to 0.97 (see Figs. 2 and 3).

Comparison of the isodensity surfaces indicated in Fig. 2S shows that the effects of substituents on the O···H and H···H interactions are negligible.

The Acidity of DPBA

The gas phase and SCRF calculations. The acidities were estimated using the ΔG values of reaction indicated in Eq. (1). The conformers of all probable anions made from the tautomers **I-III** (by removal of a proton from carboxylic, enolic and ketonic groups or change in the conformation

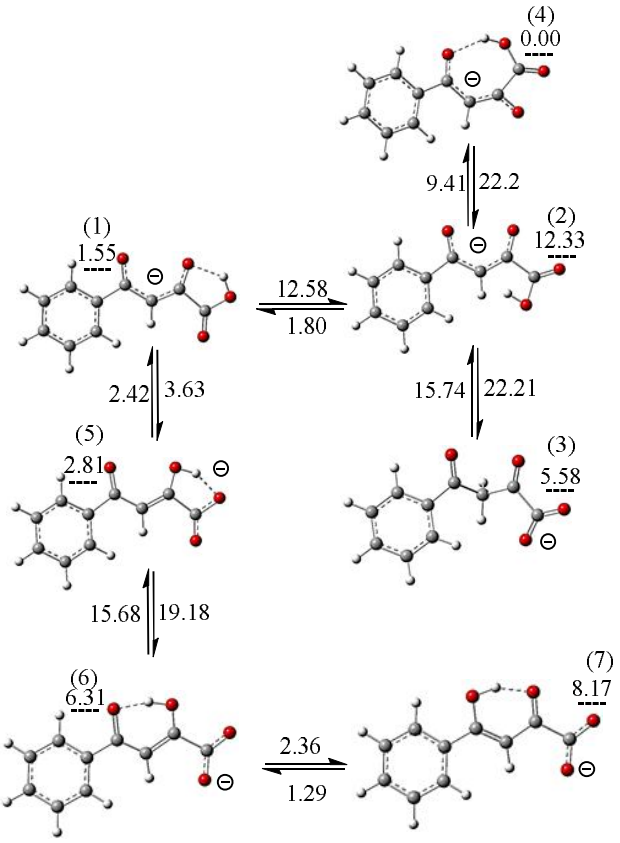

Scheme 2. The conformers of anions optimized at the M06-2X/6-311++G(d,p) level. The energy barriers are given near the arrows. The underlined data are the relative energies (relative to the up right corner conformer).

and tautomerization) are shown in Scheme 2. The conversions of conformers are performed by rotation around a bond (scanning a dihedral angle) or changing the distance between two atoms. The energy differences between various conformers are lower than 13 kcal mol^{-1} (the underlined numbers in Scheme 2 are relative energies). The energy barriers on conversions of conformers are lower than 23 kcal mol^{-1}. The trend in the stability of conformers is **4** > **1** > **5** > **3** > **6** > **7** > **2**.

The most stable conformer (as well as **1** and **2**) can be made from the removal of a proton from C5 in **I**, O1 in **II** or O2 in **III**. Three resonance structures of related anions are shown in Scheme 3.

The natural charges of O1, O2 and C5 atoms of the most stable conformer, calculated at the M06-2X/6-311++G (d,p) level, are given in Table 3S. The trend in the negative charges is O1 > O2 > C5; hence, the resonance structure **A** has the highest contribution in the electronic structure of anion, and resonance structure **B** has the lowest contribution. As can be seen in Table 3S, EDSs increase the negative charges on the mentioned atoms, and decrease the stability of anion, while EWSs behave in a reverse manner.

(a) The diketonic Tautomer **I**: the ΔG values of deprotonation process of tautomer **I**, in the gas phase and solution media, are listed in Table 4. The bold data correspond to the calculations in the solution; the data in the row indicated by H are the ΔG values of the mentioned reaction for DPBA. As can be seen, the ΔG values in the solution media are smaller than those in the gas phase. The acidity increases in the aqueous solution because the decrease in the energies of ions is larger than that of neutral species on going from gas phase to the aqueous solution. The acidity increases in the presence of EWSs such as NO_2 and halogens, and decreases in the presence of EDSs such

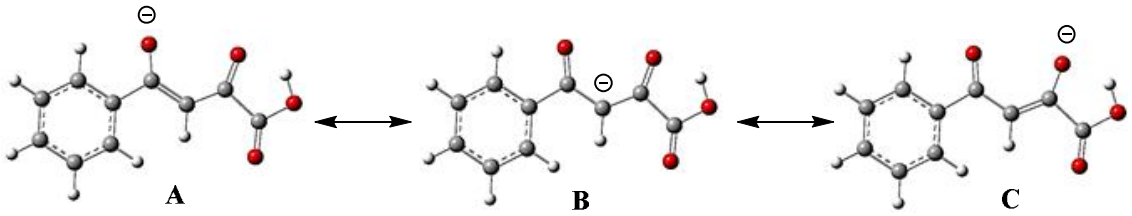

Scheme 3. The resonance of anions produced by the removal of proton from tautomers **I**, **II** and **III**

Table 4. The Relative Gibbs Free Energies (in kcal mol^{-1}) of Deprotonation Process Calculated at the M06-2X/6-311++G(d,p) Level of Theory

X	I	II		III	
NH_2	-2.41, **-1.15**	-4.43, **-3.25**	-4.16, **-2.49**	-4.23, **-2.94**	-4.01, **-2.35**
OH	-0.34, **-0.12**	-1.84, **-1.91**	-1.61, **-1.22**	0.09, **0.09**	-0.53, **-0.26**
OCH_3	-0.88, **-0.01**	-2.13, **-1.51**	-1.49, **-0.54**	-2.29, **-1.63**	-2.12, **-1.20**
CH_3	-0.86, **-0.21**	-1.53, **-0.90**	-0.54, **0.18**	-2.49, **-1.86**	-1.92, **-1.25**
F	2.58, **0.35**	2.84, **0.78**	1.96, **0.29**	2.56, **0.53**	1.79, **0.01**
Cl	3.05, **0.28**	3.91, **1.17**	3.22, **0.90**	3.14, **0.42**	1.84, **-0.51**
Br	3.37, **0.40**	4.56, **1.51**	3.52, **0.99**	4.47, **1.43**	2.84, **0.28**
CN	7.50, **1.18**	8.47, **2.07**	6.79, **1.09**	8.98, **2.62**	6.53, **0.90**
NO_2	6.50, **-0.04**	10.09, **2.94**	8.01, **0.45**	10.29, **3.17**	7.59, **1.27**
H	319.91, **166.60**	318.22, **168.91**	324.49, **167.98**	316.82, **167.82**	321.41, **166.19**

$\Delta\Delta G = \Delta G_{DPBA} - \Delta G_X$. The bold data correspond to ΔG values in the solution. The values in the latest row refer to ΔG values for DPBA. In the enolic tautomers, two columns correspond to deprotonation from positions 1 and 2, respectively.

as NH_2 and CH_3. Based on the natural charges listed in Table 3S, EWSs decrease the charges of specified atoms of anion; therefore, they stabilize the related anion and increase the acidity of compound, while EDSs behave in the opposite manner and decrease the acidity.

(b) The enolic tautomer **II**: the H1 and H2 atoms contribute in competition for deprotonation, and affect the acidity of enolic tautomer **II**. The ΔG values of deprotonation processes at the two positions 1 and 2 (ΔG_1 and ΔG_2 presented in the second and third columns) are listed in Table 4. According to those data, deprotonation from position 1 is easier than that from position 2 in the gas phase.

The OH1···O interaction is stronger than O···H2O; therefore, the occupancy of σ*OH1 antibonding orbital (0.052 e) is higher than that of σ*OH2 orbital (0.017 e) making the deprotonation easier at position 1 as compared to position 2.

On the other hand, the carboxylic group is more acidic than the enolic group in the aqueous solution. The change of dipole moment is higher on the deprotonation of carboxyl group; hence, the decrease in energy of respective anion is larger in the aqueous solution, which decreases the ΔG value and increases the acidity of corresponding functional

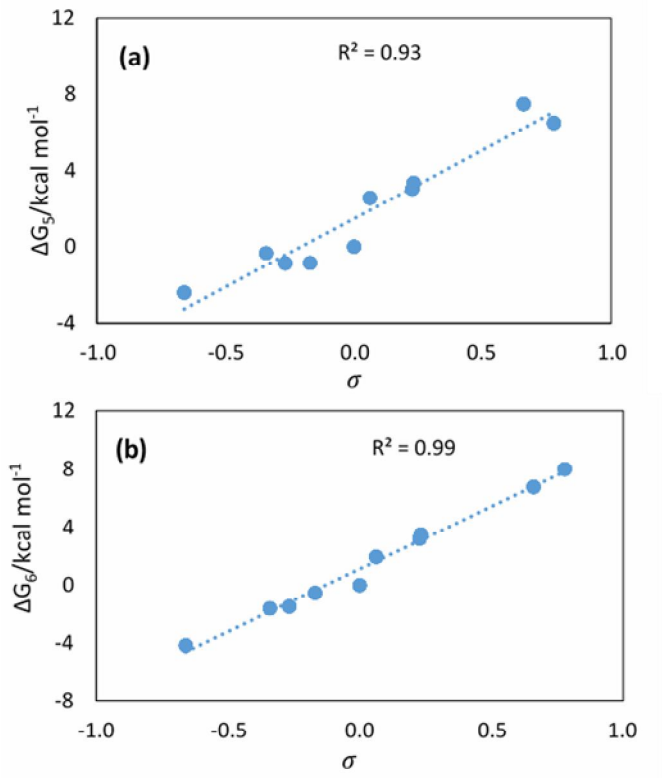

Fig. 4. Correlation between Hammett constants and (a) ΔG_1, and (b) ΔG_2 in the tautomer **II**.

group. Herein, the substituent effects on the deprotonation process are similar to those of tautomer **I**. A good linear correlation is observed between the acidities of functional groups and the σ constants of substituents (R^2 = 0.93 for position 1 and R^2 = 0.99 for position 2) in tautomer **II** (see Figs. 4a and 4b).

(c) the enolic tautomer **III**: two above-mentioned groups can also participate in the deprotonation process in the enolic tautomer **III**. Same anions are obtained on the deprotonation from the position 1 in the tautomers **II** and **III**. The ΔG values related to the removal of H^+ in the gas phase and aqueous solution are listed in Table 4. Similar to the tautomer **II**, the removal of H^+ from position 1 is easier than 2 in the gas phase, while the trend is reversed in the solution. The substituent effects on the ΔG values and the acidity of **III** are similar to those of other tautomers.

In DPBA, the ΔG values of deprotonation from the carboxyl groups of tautomers **I-III** are respectively equal to 319.91, 324.49 and 321.41 kcal mol^{-1} in the gas phase. The related values for deprotonation from the enolic groups of **II** and **III** are 318.22 and 316.82 kcal mol^{-1}, respectively. Thus, the acidity of carboxyl group in **I** is higher than those in **II** and **III**, while it is lower than those of the enolic groups of **II** and **III** in the gas phase. On the other hand, the ΔG value of deprotonation from the carboxyl group of **III** (166.19) is slightly lower than that of **I** (166.60) and **II** (167.98) in the solution.

The ΔG values of deprotonation of carboxyl and enolic groups of tautomer **II** are slightly larger than those of tautomer **III** in the gas phase and solution; therefore, the acidity of **II** is lower than **III** in both phases. This can be attributed to the higher stability of respective anions in the gas phase and solution.

Explicitly introducing the solvent molecules. Eight water molecules were located around each tautomer (see Scheme 4) in the chemically rational positions, and the structures optimized at the M06-2X/6-311++G(d,p) level in order to investigate the acidity in the presence of solvent

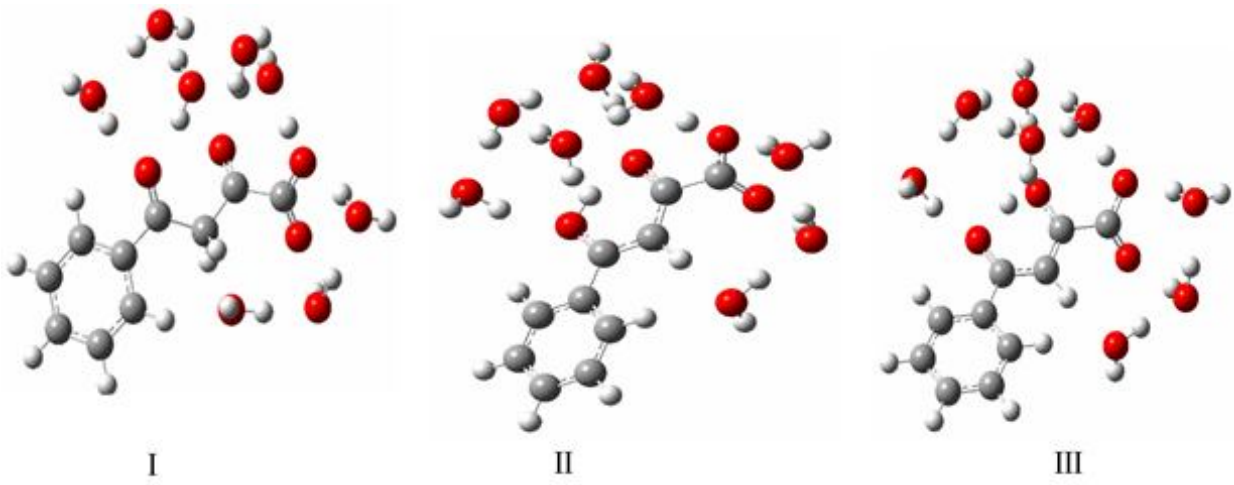

Scheme 4. The tautomers of DPBA surrounded by eight water molecules

molecules using the reaction indicated in Eq. (2).

The results obtained from scanning the distance between the H atom of carbonyl group and the O atom of the nearest water molecule are indicated in Figs. 5 and 6. As can be seen in Fig. 5a, two minima connected with a small energy barrier are observed on scanning the H atom of carboxyl group. The energy difference between the two minima is very small for the tautomers **I-III**. The energy barrier of diketo tautomer (0.81 kcal mol^{l}) is higher than those of enolic tautomers (0.12 and 0.11 kcal mol^{-1}). Comparison between plots presented in Figs. 5b-5d indicates that the energy barrier and the energy difference between the two minima do not change significantly by EDSs located at the ring, while EWSs change the pattern substantially. The complex $AH\cdots H_2O$ is generally a little less stable than $A^-\cdots H_3O^+$ in the presence of EDSs. On the other hand, the relative stability of two complexes is reversed, and no energy barrier (or a very small barrier) is observed from $A^-\cdots H_3O^+$ to $AH\cdots H_2O$ in the presence of EWSs. Therefore, the equilibrium $HA + H_2O \leftrightarrows H_3O^+ + A^-$ shifts to right by EDSs and to left by EWSs, which contradicts the impression that EWSs/EDSs can stabilize/destabilize the anions and increase/decrease the acidity of related compounds.

The results of scanning the distance between enolic hydrogen (in tautomers **II** and **III**) and the oxygen atom of the nearest water molecule are plotted in Figs. 6a-6c. Considering that the enolic tautomer is an H-acid, the left side is more stable than the right side in the above-mentioned equilibrium. No energy barrier is observed between two sides. Although the right side is not a ground stationary point, the energy difference between two sides is lower than 10 kcal mol^{-1}. As can be seen in Figs. 6b and 6c, the difference between two sides increases/decreases a little in the presence of EDSs/EWSs.

Complexation with Metal Ions

The complexation of organic compounds with the Mg^{2+}, Mn^{2+}, Ca^{2+}, Cu^{2+} and Zn^{2+} ions is physiologically important in human body [11,18]. In the present work, the complexation of the most stable conformers of tautomers **I**, **II** and **III** of DPBA with Mg^{2+} cation has been investigated in the gas phase and solution media. The structures of the most probable complexes of tautomers **I**, **II** and **III** with Mg^{2+} ion are shown in Scheme 5. As can be seen, the diketoic tautomer **I** with the nonplanar structure can bind to Mg^{2+} from three regions, and the complexation occurs from one region in the planar tautomers **II** and **III**.

The ΔG values of $AH + Mg^{2+} \rightarrow AHMg^{2+}$ process calculated in the gas phase and the solution media (AH = DPBA or one of its derivatives) are given in Scheme 5. As can be seen, the values calculated in the gas phase are more negative than those in the solution media, which may be attributed to the higher stability of Mg^{2+} in the solution. The most negative ΔG value corresponds to the diketoic tautomer **I** from the first region; the ΔG values are

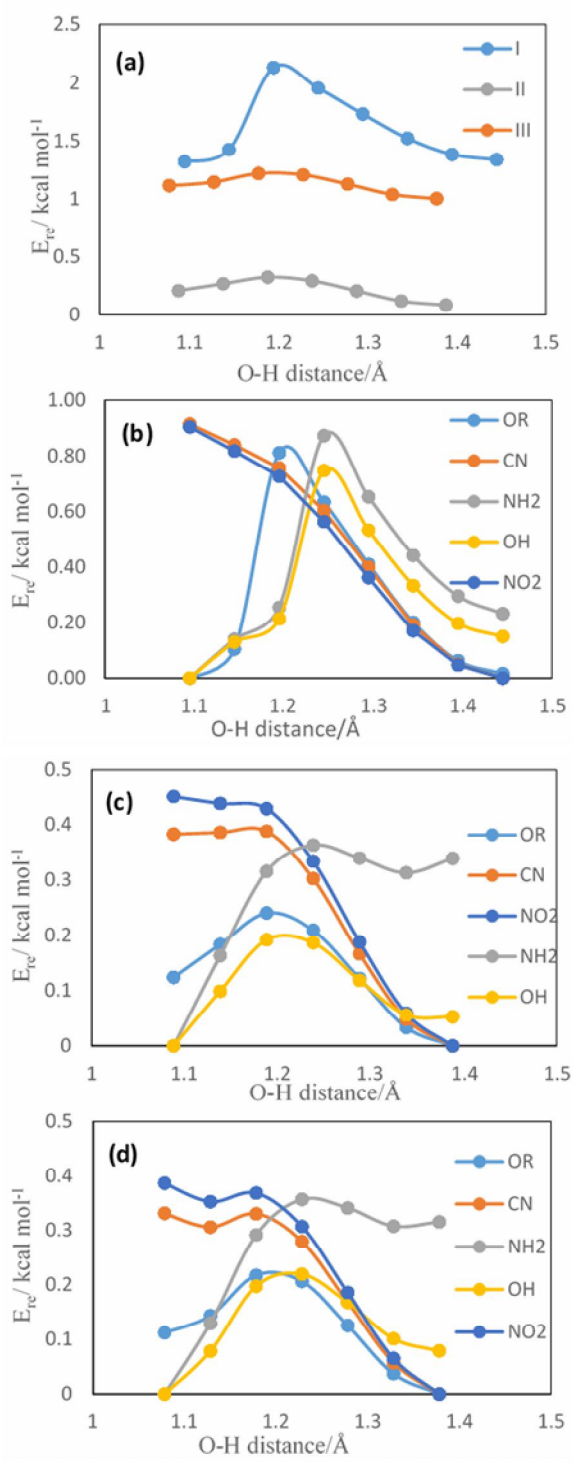

Fig. 5. The results of scanning the distance between the H atom of carboxyl group and the nearest water molecule in the (a) tautomers **I-III**, (b) substituted diketo tautomer **I** (X-**I**), (c) substituted enolic tautomer **II** (X-**II**), and (d) substituted enolic tautomer **III** (X-**III**).

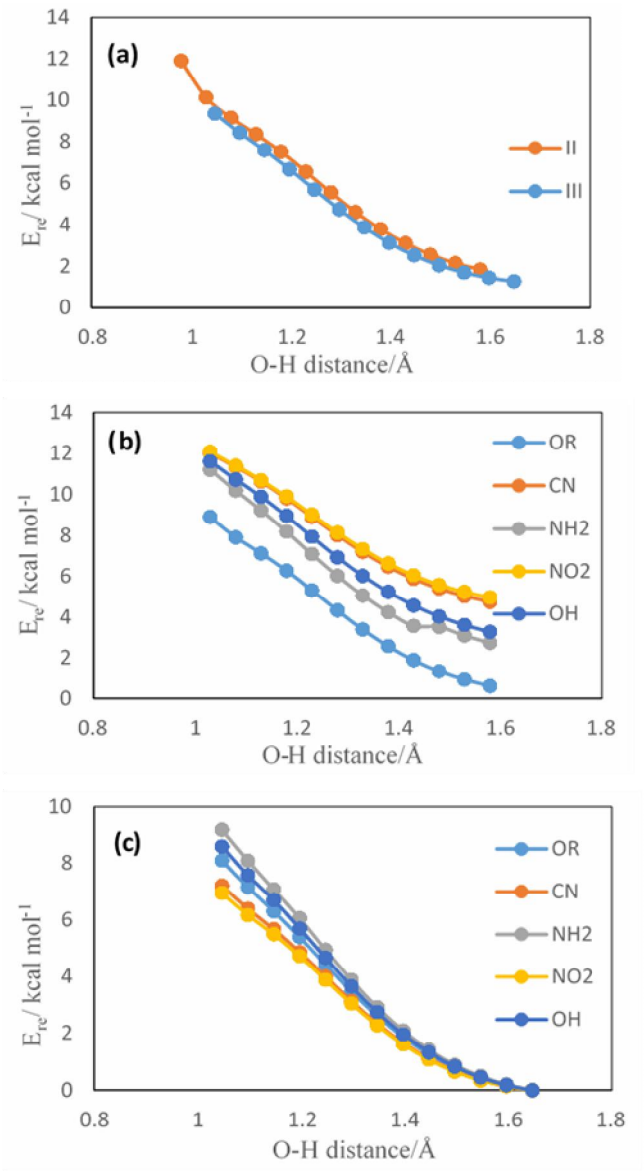

Fig. 6. The results of scanning the distance between the H atom of enolic group and the nearest water molecule in the (a) enolic tautomers **II** and **III**, (b) substituted enolic tautomer **II** (X-**II**), and (c) substituted enolic tautomer **III** (X-**III**).

-171.39, -164.94 and -125.91 kcal mol^{-1} for tautomers **I** (complex 1), **II** and **III**, respectively. The diketoic tautomer **I** has two other possibilities for complexation with Mg^{2+} (complexes 2 and 3). Approaching the oxygen atoms of region 1, which is not possible for the enolic tautomers, gives a higher tendency to tautomer **I** for complexation with Mg^{2+}.

The complexation with Mg^{2+} can affect the acidic behavior of DPBA. The ΔG values of $AH \rightarrow A^- + H^+$ and $AHMg^{2+} \rightarrow AMg^+ + H^+$ reactions, calculated at the M06-2X/6-311++G(d,p) level, are given in Table 5. Herein, AH and $AHMg^{2+}$ refer to tautomers **I-III** and their complexes, respectively. Comparison between the ΔG values of the above mentioned deprotonation processes can be used to

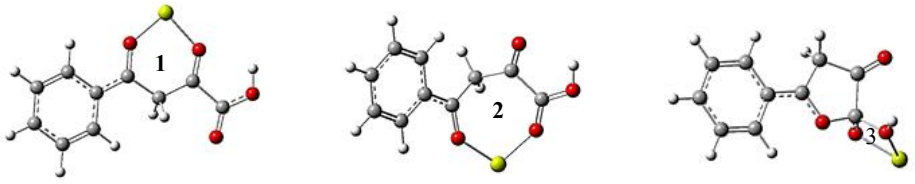

-171.39 **-6.40** -157.27 **-6.24** -145.94 **-0.16**

I-Mg^{2+}

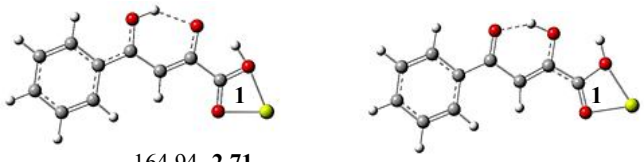

-164.94 **-2.71** -125.91 **-4.11**

II-Mg^{2+} **III-Mg^{2+}**

Scheme 5. The complexes of tautomers with the Mg^{2+} ion. The data indicated under the complexes are the ΔG values of complexation. The ΔG values obtained in the solution media are bold

Table 5. The Gibbs Free Energies (in kcal mol^{-1}) of Deprotonation Process Calculated at the M06-2X/6-311++G(d,p) Level after Complexation with Mg^{2+}

	ΔG_1	ΔG_2	ΔG_3
I	122.94 **146.61**	108.83 **159.32**	95.92 **143.45**
II	153.08 **162.81**	142.62 **145.40**	
III	112.64 **163.12**	102.13 **145.24**	

investigate the effect of complexation with Mg^{2+} on the acidic behavior of tautomers.

All data correspond to the deprotonation from carboxylic groups of complexes presented in Scheme 5 with the exception of ΔG_2 for **II** and **III** corresponding to the deprotonation from enolic group. The bold data are the ΔG values calculated in the solution.

The effect of complexation on the ΔG value depends not only on the media, but also on the type of tautomer. As can be seen in Table 5, the ΔG value of deprotonation of carboxyl group is reduced by 197-224 kcal mol^{-1} in the gas phase for tautomer **I**. The ΔG values of deprotonation from enolic and carboxyl group decrease by 176 and 171 kcal mol^{-1}, respectively, for tautomer **II** after complexation. The related changes are 215 and 209 kcal mol^{-1} for tautomer **III**. As a result, the trend in the acidity of carboxyl group remains constant (**I** > **III** > **II**) after complexation with Mg^{2+}. An exception is observed in the aqueous solution before complexation, where the ΔG value in **III** is slightly lower than that in **I**.

The ΔG value of deprotonation of tautomer **I** decreases by 7-23 kcal mol^{-1} after complexation in solution depending on the position of binding to Mg^{2+}. The related changes are approximately equal to 24 (23) and 5 (3) kcal mol^{-1} for deprotonation from the enolic and carboxylic groups, respectively, for tautomer **II** (**III**).

CONCLUSIONS

According to quantum mechanical calculations, the most stable conformers of enolic tautomers **II** and **III** of DPBA are planar that are more stable than the most stable conformer of diketonic tautomer **I** with a nonplanar structure in the gas phase and solution, where the trend of stability (**II** > **III** > **I**) is independent of the level of calculations. The strong intramolecular hydrogen bonding (C=O···H, r = 1.69-2.00 Å) and electron delocalization may be two reasons for the higher stability of enolic tautomers **II** and **III** in comparison to the diketoic tautomer **I**. The difference between the stabilities of two enolic tautomers decreases from the gas phase to the solution and with the increase in dielectric constant of solvent. It is equal to 5.20, 2.52 and 1.75 kcal mol^{-1} in the gas phase, $CHCl_3$, and water, respectively, at the M06-2X/6-311++G(d,p) level.

The enolic tautomers have two OH···O intramolecular H-bonds. Based on the geometrical parameters (r = 1.62 *vs*. 1.69 Å), and the results of NBO ($E^{(2)}$ = 34.6 *vs*. 24.3 kcal mol^{-1}) and AIM ($\rho \times 10^{-2}$ = 1.52 *vs*. 1.48 a.u.) analyses, O···H1O in **III** is stronger than OH1···O in **II** because of the effect of other H-bond, which decreases (increases) the tendency of acceptor (donor) in the OH1···O (O···H1O) of **II** (**III**). Although the O···H1 interaction in **III** is stronger than H1···O in **II**, the repulsive H···H interaction and the orientation of double bonds make **II** more stable than **III**. Depending on the functional group, the EDSs/EWSs located at the *para*-position increase/decrease the strength of intramolecular H-bond.

The difference in the stabilization energies of **II** and **III** in the presence of various substituents is less than 4.5 (2.5) kcal mol^{-1} in the gas phase (solution) and the trend in the relative stabilities does not change by substituents. However, the effects of substituents on the relative stabilities of tautomers is very small (< 0.35 kcal mol^{-1}).

The stabilities of tautomers **I** and **III** relative to **II** decrease in the presence of EWSs, while they often increase in the presence of EDSs. The σ constants of substituents are in good linear relationships (R = 0.97) with the ρ values calculated at the O···H BCPs and the $E^{(2)}$ values of lpO → σ*(OH).

The acidities of tautomers in the solution were estimated using two methods: (1) the solvent effects were considered implicitly using IEFPCM model, and (2) eight water molecules were located at the chemically rational positions around each tautomer. In both methods, the calculated thermodynamic properties of deprotonation process show that the acidity of diketo tautomer **I** is comparable with those of enolic tautomers **II** and **III** in the gas phase and solution. The ΔG values of deprotonation of tautomers **I-III** of DPBA decrease from 319.91, 324.49 and 321.41 in the gas phase to 166.60, 167.98 and 166.19 kcal mol^{-1} in the solution. In tautomers **II** and **III**, the enolic functional group has a higher acidity compared to the carboxylic group in the gas phase**,** but it is reversed in the aqueous solution (independent of considering the effects of solvent molecules explicitly or implicitly) and after complexation with Mg^{2+}. Depending on the functional group, the ED/EW substituents located at the para-position decrease/increase the acidity.

The tendency of several sites of DPBA for complexation with Mg^{2+} has been investigated at the gas phase and solution. The diketoic tautomer **I** with a nonplanar structure can bind to Mg^{2+} from three regions, and complexation occurs from one region in planar tautomers **II** and **III**. The ΔG values of complexation of tautomers **I** (and complexes **2** and **3**), **II** and **III** change from -171.39 (-157.27, -145.94), -164.94 and -125.91 in the gas phase to -6.40 (-6.24, -0.16), -2.71 and -4.11 kcal mol^{-1} in the solution, respectively.

The trend in the acidity of carboxyl group remains constant (**I** > **III** > **II**) after complexation with Mg^{2+}. An exception is observed in the aqueous solution before complexation, where the ΔG value in **III** is slightly lower than that in **I**.

The ΔG value of deprotonation of carboxyl group decreases by 7-23, 5 and 7 kcal mol^{-1} in solution in tautomers **I-III**, respectively, after complexation; the related change for the enolic group in **II** and **III** is 24 and 23 kcal mol^{-1}. Although the acidity is substantially higher in the aqueous solution, the change in acidity by complexation in the aqueous solution is substantially lower than that in the gas phase.

ACKNOWLEDGMENTS

We thank the University of Sistan and Baluchestan for scientific supports and Computational Quantum Chemistry Laboratory for computational facilities.

REFERENCES

[1] Podolesov, B. D.; Jordanovska, V. B.; Korunoski, M. R.; Tosev, D. N., Reaction of titanium(IV) chloride with the ethyl esters of some β-diketo acids, *J. Inorg. Nucl. Chem.,* **1974**, *36*, 1495-1497. DOI: 10.1016/0022-1902(74)80612-3.

[2] Moriarty, R. M.; Vaid, R. K.; Hopkins, T. E.; Vaid, B. K.; Prakash, O., Hypervalent iodine oxidation of 5-keto acids and 4,6-diketo acids with [hydroxy(tosyloxy)iodo]benzene: Synthesis of keto-γ-lactones and diketo-δ-lactones, *Tetrahedron Lett.,* **1990**, *31*, 201-204. DOI: 10.1016/S0040-4039(00)94370-3.

[3] Cvijetic, I. N.; Verbic, T. Z.; de Resende, P. E.; Stapleton, P.; Gibbons, S.; Juranic, I. O.; Drakulic, B. J.; Zloh, M., Design, synthesis and biological evaluation of novel aryldiketo acids with enhanced antibacterial activity against multidrug resistant bacterial strains, *Eur. J. Med. Chem.,* **2018**, *143*, 1474-1488. DOI: 10.1016/j.ejmech.2017.10.045.

[4] Summa, V.; Petrocchi,A.; Pace,P.; Matassa,V. G.; De Francesco, R.; Altamura, S.; Tomei, L.; Koch, U.; Neuner, P., Discovery of α,γ-diketo acids as potent selective and reversible inhibitors of hepatitis C Virus NS5b RNA-dependent RNA polymerase, *J. Med. Chem.,* **2004**, *47*, 14-17. DOI: 10.1021/jm0342109.

[5] Kozlov, M. V.; Polyakov, K. M.; Filippova, S. E.; Evstifeev, V. V.; Lyudva, G. S.; Kochetkov, S. N., RNA-dependent RNA polymerase of hepatitis C virus: study on inhibition by α,γ-diketo acid derivatives, *Biochem. (Moscow),* **2009**, *74*, 834-841. DOI: 10.1134/S0006297909080033.

[6] Studer, M.; Burkhardt, S.; Indolese, A. F.; Blaser, H. U., Enantio- and chemoselective reduction of 2,4-diketo acid derivatives with cinchona modified Pt-catalyst-synthesis of (R)-2-hydroxy-4-phenylbutyric acid ethyl ester, Chem. Commun., 2000, 0, 1327-1328. DOI: 10.1039/B002538K.

[7] Dayam, R.; Sanchez, T.; Neamati, N., Diketo acid pharmacophore. 2. Discovery of structurally diverse inhibitors of HIV-1 integrase, *J. Med. Chem.,* **2005**, *48*, 8009-8015. DOI: 10.1021/jm050837a.

[8] Santo, R. D.; Costi, R.; Roux, A.; Artico, M.; Lavecchia, A.; Marinelli, L.; Novellino, E.; Palmisano, L.; Andreotti, M.; Amici, R.; Galluzzo, C. M.; Nencioni, L.; Palamara, A. T.; Pommier,Y.; Marchand, C., Novel bifunctional quinolonyl diketo acid derivatives as HIV-1 integrase inhibitors: design, *J. Med. Chem.,* **2006**, *49*, 1939-1945. DOI: 10.1021/jm0511583.

[9] Sechi, M.; Bacchi, A.; Carcelli, M.; Compari, C.; Duce, E.; Fisicaro, E.; Rogolino, D.; Gates, P.; Derudas, M.; Al-Mawsawi, L. Q.; Neamati, N., From ligand to complexes: inhibition of human immunodeficiency virus type 1 integrase by β-diketo acid metal complexes, *J. Med. Chem.,* **2006**, *49*, 4248-4260. DOI: 10.1021/jm060193m.

[10] Uchil,V.; Seo, B.; Nair, V., A novel strategy to assemble the β-diketo acid Pharmacophore of HIV integrase inhibitors on purine nucleobase scaffolds, *J. Org. Chem.,* **2007**, *72*, 8577-8579. DOI: 10.1021/jo701336r.

[11] Santo, R. D.; Costi, R.; Roux, A.; Miele, G.; Crucitti, G. C.; Iacovo, A.; Rosi, F.; Lavecchia, A.; Marinelli, L.; Giovanni, C. D.; Novellino, E.; Palmisano, L.; Andreotti, M.; Amici, R.; Galluzzo, C. M.; Nencioni, L.; Palamara, A. T.; Pommier, Y.; Marchand, C., novel quinolinonyl diketo acid derivatives as HIV-1 integrase inhibitors: design, synthesis, and biological activities, *J. Med. Chem.,* **2008**, *51*, 4744-4750. DOI: 10.1021/jm8001422.

[12] Bacchi, A.; Biemmi, M.; Carcelli, M.; Carta, F.; Compari, C.; Fisicaro, E.; Rogolino, D.; Sechi, M.; Sippel, M.; Sotriffer, C. A.; Sanchez, T. W.; Neamati, N., From ligand to complexes. part 2 remarks on Human Immunodeficiency Virus type 1 integrase inhibition by β-diketo acid metal complexes, *J. Med. Chem.,* **2008**, *51*, 7253-7264. DOI: 10.1021/jm800893q.

[13] Alves, C. N.; Marti, S.; Castillo, R.; Andres, J.; Moliner, V.; Tunon, I.; Silla, E., A quantum mechanic/molecular mechanic study of the wild-type and N155S mutant HIV-1 integrase complexed with diketo acid, *Biophys. J.,* **2008**, *94*, 2443–2451. DOI: 10.1529/biophysj.107.107623.

[14] Costi, R.; Métifiot, M.; Chung, S.; Crucitti, G. C.; Maddali, K.; Pescatori, L.; Messore, A.; Madia, V. N.;

Pupo, G.; Scipione, L.; Tortorella, S.; Leva, F. S. D.; Cosconati, S.; Marinelli, L.; Novellino, E.; Grice, S. F. J. L.; Corona, A.; Pommier, Y.; Marchand, C.; Santo, R. D., Basic quinolinonyl diketo acid derivatives as inhibitors of HIV integrase and their activity against RNase H function of reverse transcriptase, *J. Med. Chem.,* **2014**, *57*, 3223-3234. DOI: 10.1021/jm5001503.

[15] Poongavanam, V.; Hari, N. S.; Moorthy, N.; Kongsted, J., Dual mechanism of HIV-1 integrase and RNase H inhibition by diketo derivatives, a computational study, *RSC Adv.,* **2014**, *4*, 38672-38681. DOI: 10.1039/C4RA05728G.

[16] Pescatori, L.; Métifiot, M.; Chung, S.; Masoaka, T.; Crucitti, G. C.; Messore, A.; Pupo, G.; Madia, V. N.; Saccoliti, F.; Scipione, L.; Tortorella, S.; Leva, F. S. D.; Cosconati, S.; Marinelli, L.; Novellino, E.; Grice, S. F. J. L.; Pommier, Y.; Marchand, C.; Costi, R.; Santo, R. D., N-substitued quinolinonyl diketo acid derivatives as HIV integrase strand transfer inhibitors and their activity against RNase H function of reverse transcriptase, *J. Med. Chem.,* **2015**, *58*, 4610-4623. DOI: 10.1021/ acs.jmedchem.5b00159.

[17] Crucitti, G. C.; Métifiot, M.; Pescatori, L.; Messore, A.; Madia, V. N.; Pupo, G.; Saccoliti, F.; Scipione, L.; Tortorella, S.; Esposito, F.; Corona, A.; Cadeddu, M.; Marchand, C.; Pommier, Y.; Tramontano, E.; Costi, R.; Santo, R. D., Structure-activity relationship of pyrrolyl diketo acid derivatives as dual inhibitors of HIV-1 integrase and reverse transcriptase ribonuclease H domain, *J. Med. Chem.,* **2015**, *58*, 1915-1928. DOI: 10.1021/jm501799k.

[18] Han, D.; Su, M.; Tan, J.; Li, C.; Zhang, X.; Wang, C., Structure-activity relationship and binding modes studies for a series of diketo-acids as HIV integrase inhibitors by 3D-QSAR, molecular docking and molecular dynamics simulations, *RSC. Advances* **2016**, *6*, 27594-27606. DOI: 10.1039/C6RA00713A.

[19] Nair, V.; Uchil, V.; Neamati, N., β-diketo acids with purine nucleobase scaffolds: Novel, selective inhibitors of the strand transfer step of HIV integrase, *Bioorg. Med. Chem. Lett.,* **2006**, *16*, 1920-1923. DOI: 10.1016/ j.bmcl.2005.12.093.

[20] Yoshinaga, T. S.; Fujishita, T.; Fujiwara, T., *In vitro* activity of a new HIV-1 integrase inhibitor in clinical development. Presented at the 9th conference on retroviruses and opportunistic infections, 2002 February 24- 28; Seattle, WA.

[21] Young, S. L., A potent antiviral HIV integrase inhibitor with potential clinical utility. Presented at the XIV international AIDS conference, 2002 July 7-12, West Point, PA, USA.

[22] Hazuda, D. J.; Felock, P.; Witmer, M.; Wolfe, A.; Stillmock, K.; Grobler, J. A.; Espeseth, A.; Gabryelski, L.; Schleif, W.; Blau, C.; Miller, M. D., Inhibitors of strand transfer that prevent integration and inhibit HIV-1 replication in cells, *Science,* **2000**, *287*, 646-650. DOI: 10.1126/science.287.5453.646.

[23] Hazuda, D. J.; Young, S. D.; Guare, J. P.; Anthony, N. J.; Gomez, R. P.; Wai, J. S.; Vacca, J. P.; Tussey, L.; Handt, S. L.; Motzel, H. J.; Klein, G.; Dornadula, R. M.; Danovich, M. V.; Witmer, K. A.; Wilson, L.; Schleif, W. A.; Gabryelski, L.; Miller, M. D.; Casimiro, D. R.; Emini, E. A.; Shiver, J. W., Integrase inhibitors and cellular immunity suppress retroviral replication in rhesus macaques, *Science,* **2004**, *305*, 528-532. DOI: 10.1126/science.1098632.

[24] Santo, R. D.; Fermeglia, M.; Ferrone, M.; Paneni, M. S.; Costi, R.; Artico, M.; Roux, A.; Gabriele, M.; Tardif, K. D.; Siddiqui, A.; Pricl, S., Simple but highly effective three-dimensional chemical-feature-based pharmacophore model for diketo acid derivatives as Hepatitis C virus RNA-dependent RNA polymerase inhibitors, *J. Med. Chem.,* **2005**, *48*, 6304-6314. DOI: 10.1021/jm0504454.

[25] Kozlov, M. V.; Polyakov, K. M.; Ivanov, A. V.; Filippova, S. E.; Kuzyakin, A. O.; Tunitskaya, V. L.; Kochetkov, S. N., Hepatitis C virus RNA-dependent RNA polymerase: study on the inhibition mechanism by pyrogallol derivatives, *Biochem. (Moscow),* **2006**, *71*, 1021-1026. DOI: 10.1134/S0006297906090112.

[26] Deore, R. R.; Chen, G. S.; Chang, P. -T.; Chern, T. -R.; Lai, S. -Y.; Chuang, M. -H.; Lin, J. -H.; Kung, F. -L.; Chen, C. -S.; Chiou, C. -T.; Chern, J. -W., Discovery of N-arylalkyl-3-hydroxy-4-oxo-3,4-dihydroquinazolin-2-carboxamide derivatives as HCV NS5B polymerase inhibitors, *Chem. Med. Chem.* **2012**, *7*, 850-860. DOI: 10.1002/ cmdc.201200058.

[27] Oxford, J. S.; Lambkin, R., Targeting influenza virus neuraminidase a new strategy for antiviral therapy, *Drug Discov. Today,* **1998**, *3*, 448-456. DOI: 10.1016/S1359-6446(98)01241-0.

[28] Dias, A.; Bouvier, D. Crepin, T.; McCarthy, A. A.; Hart, D. J.; Baudin, F.; Cusack, S.; Ruigrok, R. W. H., The cap-snatching endonuclease of influenza virus polymerase resides in the PA subunit, *Nature,* **2009**, *458*, 914-918. DOI: 10.1038/nature07745.

[29] Reguera, J.; Weber, F.; Cusack, S., Bunyaviridae RNA polymerases (L-protein) have an N-terminal, influenza-like endonuclease domain, essential for viral cap-dependent transcription, *Plos Pathog.,* **2010**, *6*, 1-14. DOI: 10.1371/journal.ppat.1001101.

[30] Tran, N.; Tran. L.; Le, L., Strategy in structure-based drug design for influenza a virus targeting M2 channel proteins, *Med. Chem. Res.,* **2013**, *22*, 6078-6088. DOI: 10.1007/s00044-013-0599-z.

[31] Bauzá, A.; Quiñonero, D.; Deyà, P. M.; Frontera, A., Long-Range effects in anion-π interactions: their crucial role in the inhibition mechanism of mycobacterium tuberculosis malate synthase, *Chem. Eur. J.,* **2014**, *20*, 6985-6990. DOI: 10.1002/chem.201304995.

[32] Cvijeti, I. N.; Verbi, T. Z.; Drakuli, B. J.; Stankovi, D. M.; Jurani, I. O.; Manojlovi, D. D.; Zloh, M., Redox properties of alkyl-substituted 4-aryl-2,4-dioxo-butanoic acids, *J. Serb. Chem. Soc.,* **2017**, *82*, 303-316. DOI: 10.2298/JSC161118021C.

[33] Verbić, T. Ž.; Zloh, M. F.; Stanković, D. M.; Sentić, M. M.; Manojlović, D. D.; Juranić, I. O., In Proceedings of the 49th Meeting of the Serbian Chemical Society, Kragujevac, Serbia, 2011, p. 16.

[34] Jeffrey, G. A., An introduction to hydrogen bonding, Oxford University Press, New York, 1997.

[35] Grabowski, S. J., Challenges and advances in computational chemistry and physics. Vol. 3, Hydrogen bonding – New Insights, Springer, Berlin, 2006.

[36] Gilli, G.; Bellucci, F.; Ferretti, V.; Bertolasi, V., Evidence for resonance-assisted hydrogen bonding from crystal-structure correlations on the enol form of the β-diketone fragment, *J. Am. Chem. Soc.,* **1989**, *111*, 1023-1028. DOI: 10.1021/ja00185a035.

[37] Sanz, P.; Mó, O.; Yáñez, M.; Elguero, J., Resonance-assisted hydrogen bonds: a critical examination. Structure and stability of the enols of β-diketones and β-enaminones, *J. Phys. Chem. A,* **2007**, *111*, 3585-3591. DOI: 10.1021/jp067514q.

[38] Estarellas, C.; Frontera, A.; Quiñonero, D.; Deyà, P. M., Interplay between cation-π and hydrogen bonding interactions: Are non-additivity effects additive?, *Chem. Phys. Lett.,* **2009**, *479*, 316-320. DOI: 10.1016/j.cplett.2009.08.035.

[39] Wu, J. I.; Jackson, J. E.; Rague Schleyer, P., Reciprocal hydrogen bonding-aromaticity relationships, *J. Am. Chem. Soc.,* **2014**, *136*, 13526-13529. DOI: 10.1021/ja507202f.

[40] Schroder, S. D.; Wallberg, J. H.; Kroll, J. A.; Maroun, Z.; Vaida, V.; Kjaergaard, H. G., Intramolecular hydrogen bonding in methyl lactate, *J. Phys. Chem. A,* **2015**, *119*, 9692-9702. DOI: 10.1021/acs.jpca.5b04812.

[41] Moosavi-Tekyeh, Z.; Taherian, F.; Tayyari, S. F., Intramolecular hydrogen bonding in 5 nitrosalicylaldehyde: IR spectrum and quantum chemical calculations, *J. Mol. Struc.,* **2016**, *1111*, 185-192. DOI: 10.1016/j.molstruc.2016.01.084.

[42] Darugar, V. R.; Vakili, M.; Nekoei, A. R.; Tayyari, S. F.; Afzali, R., Tautomerism, molecular structure, intramolecular hydrogen bond, and enol-enol equilibrium of para halo substituted 4,4,4-trifluoro-1-phenyl-1,3-butanedione; Experimental and theoretical studies, *J. Mol. Struc.,* **2017**, *1150*, 427-437. DOI: 10.1016/j.molstruc.2017.09.004.

[43] Yang, J.; Li, A. Y., Hydrogen bond strengthening between o-nitroaniline and formaldehyde in electronic excited states: A theoretical study, *Spectrochim. Acta Part A: Mol. and Biomol. Spectrosc.,* **2018**, *199*, 194-201. DOI: 10.1016/j.saa.2018.03.062.

[44] Alkorta, I.; Elguero, J.; Mo´, Manuel Yáñez, O.; Del Bene, J. E., Are resonance-assisted hydrogen bonds'resonance assisted'? A theoretical NMR study, *Chem. Phys. Lett.,* **2005**, *411*, 411-415. DOI: 10.1016/j.cplett.2005.06.061.

[45] Trujillo, C.; Sánchez-Sanz, G.; Alkorta, I.; J., Mó, Manuel Yáñez, O., Resonance assisted hydrogen bonds in open-chain and cyclic structures of

malonaldehyde enol: A theoretical study, *J. Mol. Struc.,* **2013**, *1048*, 138-151. DOI: 10.1016/j.molstruc.2013.04.069.

[46] Nowroozi, A.; Jalbout, A. F.; Roohi, H.; Khalilinia, E.; Sadeghi, M.; Deleon, A.; Raissi, H., Hydrogen Bonding in Acetylacetaldehyde: Theoretical Insights from the theory of atoms in molecules, *Int. J. Quant. Chem.,* **2009**, *109*, 1505-1514. DOI: 10.1002/qua.21830.

[47] Landry, B. R.; Turnbull, M. M.; Twamley, B., Synthesis and structure of a novel copper(II) nitrate complex of 2,4-dioxo-4-phenylbutanoic acid, *J. Chem. Crystallogr.,* **2007**, *37*, 81-86, DOI: 10.1007/s10870-006-9098-0.

[48] Momeni, Z.; Ebrahimi, A., Investigation of the effect of π•••π stacking interaction on the properties of -$CONH_2$ functional group of benzamide, *Struct. Chem.,* **2015**, *27*, 731-737. DOI: 10.1007/s11224-015-0615-7.

[49] Curpana, R.; Avrama, S.; Vianellob, R.; Bologa, C., Exploring the biological promiscuity of high-through screening hits through DFT calculations, Bioorg. Med. Chem., **2014**, *22*, 2461-2468. DOI: 10.1016/j.bmc.2014.02.055.

[50] Balakrishnan, C.; Subha, L.; Neelakantan, M. A.; Mariappan, S. S., Synthesis, spectroscopy, X-ray crystallography, DFT calculations, DNA binding and molecular docking of a propargyl arms containing Schiff base, Spectrochim. Acta, Part A, **2015**, *150*, 671-681, DOI: 10.1016/j.saa.2015.06.013.

[51] Mansour, A. M., Tazarotene copper complexes: Synthesis, crystal structure, DFT and biological activity evaluation, polyhedron, **2016**, *109*, 99-106. DOI: 10.1016/j.poly.2016.01.041.

[52] Azizi, A.; Ebrahimi, A., The X^-…benzohydrazide complexes: the interplay between anion- π and H-bond interactions, *Struct. Chem.,* **2016**, *28*, 687-695. DOI: 10.1007/s11224-016-0839-1.

[53] Sarhadinia, S.; Ebrahimi, A., H-bond and dipole-dipole interactions between water and -COO- functional group in methyl benzoate derivatives: Substituent and heteroatom effects, *J. Mol. Graph. Model.,* **2016**, *70*, 7-13. DOI: 10.1016/j.jmgm.2016.09.003.

[54] Nepal, B.; Scheiner, S., Microsolvation of anions by molecules forming CH···X- hydrogen bonds, Chem. *Phys.,* **2015**, *463*, 137-144. DOI: 10.1016/j.chemphys.2015.10.013.

[55] Zhao, Y.; Schultz, N. E.; Truhlar, D. G., Design of density functionals by combining the method of constraint satisfaction with parametrization for thermochemistry, thermochemical kinetics, and noncovalent interactions. *J. Chem. Theory Comput.,* **2006**, *2*, 364-382. DOI: 10.1021/ct0502763.

[56] Frisch, M. J.; Trucks, G. W.; Schlegel, H. B., *et al.,* Gaussian 09, Revision A.02, Gaussian, Inc., Wallingford, CT, 2009.

[57] Grimme, S.; Ehrlich, S.; Goerigk, L., *J. Comput. Chem.,* **2011**, *32*, 1456-65. DOI: 10.1002/jcc.21759.

[58] Chai, J. D.; Head-Gordon, M., *Phys. Chem. Chem. Phys.,* **2008**, *10*, 6615-20. DOI: 10.1039/b810189b.

[59] a) Møller, C.; Plesset, M. S., *Phys. Rev.,* **1934**, *46*, 618. DOI: 10.1103/PhysRev.46.618.; b) Binkley, J. S.; Pople, J. A., *Int. J. Quantum Chem.,* **1975**, *9*, 229. DOI: 10.1002/qua.560090204.

[60] Bader, R. F. W., Atoms in Molecules: A Quantum Theory, Oxford University Press, Oxford, 1990.

[61] Biegler, K. F.; Schonbohm, J.; Bayles, D., AIM2000-A program to analyze and. visualize atoms in molecules, *J. Comput. Chem.,* **2001**, *22*, 545-559. DOI: 10.1002/1096-987X(20010415).

[62] Glendening, E. D.; Reed, A. E.; Carpenter, J. E.; Weinhold, F., NBO version 3.1, Theoretical Chemistry Institute, University of Wisconsin, Madison, 1990.

[63] Tomasi, J.; Mennucci, B.; Cances, E., The IEF version of the PCM solvation method: an overview of a new method addressed to study molecular solutes at the QM *ab initio* level, *J. Mol. Struct. THEOCHEM,* **1999**, *464*, 211-226. DOI: 10.1016/S0166-1280(98)00553-3.

[64] Mohajeri, A.; Omidvar, A.; Setoodeh, H., Fine structural tuning of thieno[3,2-b]pyrrole donor for designing banana-shaped semiconductors relevant to organic field effect transistors, *J. Chem. Information and Modeling,* **2018**, DOI: 10.1021/acs.jcim.8b00738.

[65] Góra, R. W.; Maj, M.; Grabowski, S. J., Resonance-

assisted hydrogen bonds revisited. Resonance stabilization vs. charge delocalization, *Phys. Chem. Chem. Phys.,* **2013**, *15*, 2514-2522. DOI: 10.1039/C2CP43562D.

[66] Hansch, C.; Leo, A.; Taft, R. W., A survey of Hammett substituent constant and resonance and field parameters, *Chem. Rev.,* **1991**, *91*, 165-195. DOI: 10.1021/cr00002a004.